2013 IEEE/RSJ International Conference on
Intelligent Robots and Systems (IROS)
November 3-7, 2013. Tokyo, Japan

Characteristics of Controllable Adhesion using Magneto-Rheological Fluid and its Application to Climbing Robotics

Masaaki Watanabe*1, Nicholas Wiltsie*2, Annette E. Hosoi*3 and Karl Iagnemma*4

Abstract— **In order to grasp and hold uneven or dusty objects, a robust adhesion mechanism is required. This paper evaluates controllable adhesion using magneto-rheological fluid (MRF) as a technique to stick to non-magnetic materials and rough/dusty surfaces. This technique is both simple to use and robust to uncertain surface conditions, as it involves applying MRF on a surface and activating it with a magnetic field. In this paper, we experimentally evaluate yield stresses in both normal and shear directions with respect to MRF layer thickness, magnetic flux density and surface type. Based on these results, a four-legged climbing robot is designed to demonstrate scaling vertical walls and shows effectiveness of the controllable adhesion using MRF for rough surface.**

I. INTRODUCTION

Many cleaning and inspection tasks on buildings, towers, or large machinery are hazardous or difficult for humans to perform. Climbing robots could reduce the danger, but any adhesion mechanism utilized in real-world scenarios must be capable of traversing uncertain, dirty, and varied surfaces such as glass, acrylic, brick, concrete, or wood.

Many robotic adhesion mechanisms have taken inspiration from biology. Sitti *et al.*[1] and Santos *et al.*[2] developed a nano / micro adhesion mechanism inspired by geckos. These robots have many soft micro-structures, creating a dry adhesive capable of passively adhering to smooth and non-dusty surface. Spenko *et al.*[3] also proposed a climbing mechanism for rough and wooden surfaces by using biologically inspired hooks like beetle's legs. Hook legs, however, require either a soft or rough surface for adhesion, and work best when the hook size is tuned to the characteristic feature size of the wall.

Other climbing technologies using non-biologically inspired methods also have been proposed. Daltorio *et al.*[4] proposed a climbing mobile robot with sticky paddles extending from wheels. This method directly adheres to surface strongly using double side tape; however, the tape is easily fouled in dusty environments and requires continual replacement. Prahlad *et al.*[5] demonstrated robotic climbing using electro-adhesives, which function by inducing an electrostatic force between the wall and the adhesive surfaces. These electro-adhesives function well in dusty and rough environments but required high voltage supplies, which may require a tether or a complex on-board power converter. Kitai *et al.*[6] proposed an investigation robot for huge iron ships. This robot sticks onto the ship body with magnetic force, so its application is limited to ferromagnetic materials such as iron or cobalt. Nagakubo *et al.*[7] developed a robot with arrayed suction cups on each foot to climb on the exterior walls of buildings. These suction cups can generate strong adhesive forces, but require a large power supply to run an external vacuum pump and are most effective on smooth surfaces. Yoshida *et al.*[8] developed a track robot with passive suction cups. This mechanism does not require a vacuum pump, but its application is strongly restricted to smooth surface.

The adhesion based on magneto-rheological fluid (MRF) discussed in this paper is unique in that it can potentially be applied to a wide range of surfaces (i.e. substrates and rough surfaces with or without dust and other surface contaminants) and yield large clamping pressures without needing a ferrous substrate or a large external power supply. Fig. 1 shows some examples of the MRF adhesion technique with a simple robotic foot. By applying a magnetic field using the movable magnet mechanism shown in Fig. 1(a), a thin layer of MRF spread between the mechanism and surface is activated and generates an adhesive force. In Fig. 1(b) and Fig. 1(c), the mechanism sticks to a vertical wooden board and hangs from an inverted board with an additional 200 g weight. When the MRF is deactivated by actuating the magnet away from the surface, the mechanism falls immediately, demonstrating the controllable nature of the adhesion. As the MRF is applied to the surface in a liquid state, it is able to absorb dust and conform to rough surfaces. In addition, once the magnet has been moved into position to activate the fluid, no further energy is required to maintain the adhesive effect.

The basic characteristics of this controllable adhesion are reported by Ewoldt *et al.*[9]. MRF consists of micron-sized iron particles suspended in a carrier fluid. As seen in Fig. 2, this particles are normally distributed randomly, but when an external magnetic field is applied the particles chain together in the direction of the field. These chains act to resist flow of the carrier fluid, increasing the viscosity of the MRF and eventually turning the fluid into a Bingham plastic with a

This research was supported by Battelle, and by DARPA under contract number W911NF-11C-0201.

*1He is with Robotics Group of IHI Corporation, 1 Shin-Nakahara-Cho, Isogo-ku, Yokohama 235-8501, JAPAN, masaaki_watanabe_2@ihi.co.jp *2He is with the Robotics Division of the Jet Propulsion Laboratory, 4800 Oak Grove Drive, Pasadena, CA, 91109, USA, nicholas.wiltsie@jpl.nasa.gov *3She is with Hatsopoulos Microfluids Laboratory, Department of Mechanical Engineering, Massachusetts Institute of Technology, 77 Massachusetts Avenue, Cambridge, MA 02139, USA, peko@mit.edu *4He is with Robotic Mobility Group, Massachusetts Institute of Technology, 77 Massachusetts Avenue, Cambridge, MA 02139, USA, masaakiw@mit.edu and kdi@mit.edu

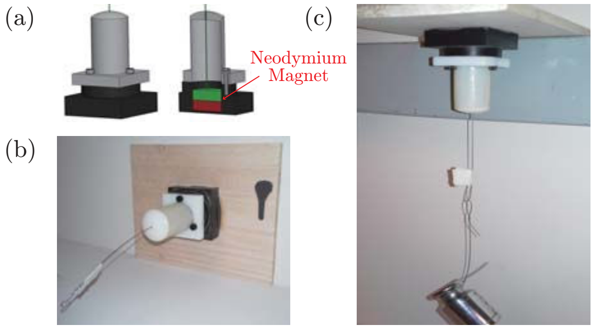

Fig. 1. Demonstrations of adhesion using MRF and Neodymium magnet on rough wooden plate. The black sole has an area of 14.5 cm^2. The neodymium magnet is 1.9 cm wide and 0.6 cm thick and generates a flux density of 0.6 T.

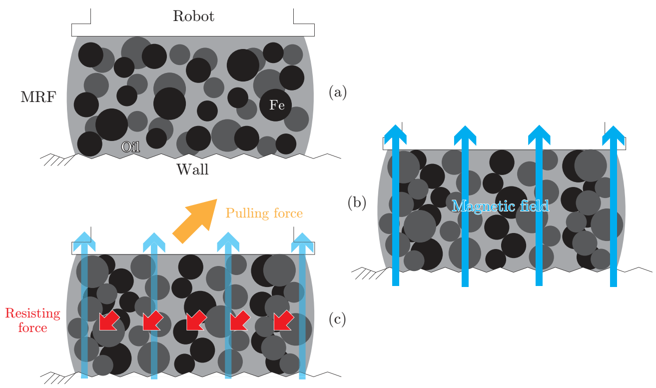

Fig. 2. Illustration of iron particles in non-activated and activated MRF.

characteristic yield stress. By using this technology, Wiltsie *et al.*[10] initially reported values of normal stresses for various MRF thicknesses with fixed flux density. However, some other factors are still unclear to get an optimal configuration for climbing technology.

In this paper, we aim to reveal characteristics of field-activated MRF this new climbing method with low energy consumption on non-smooth surfaces. In particular we focus on normal and shear yield stresses with relationships between various parameters (i.e. MRF thicknesses, magnetic field densities and surface conditions). Based on these characteristics, a new climbing robot for climbing uneven surfaces is designed and the effectiveness of this technology is demonstrated by experiment.

II. Normal stress test

A. Measurement device and its model

The probe-tack machine and electromagnet shown in Fig. 3 were used to measure the adhesive normal stress of the MRF as a function of applied field density and fluid thickness. The electromagnet generated magnetic fluxes between 0 and 0.25 T in this experiment by supplying between 0 and 4 A from a DC power supply. The probe-tack machine was capable of measuring and recording forces along the vertical axis between 0 and 250 N. Fig. 4 shows a model of normal stress test. The MRF used in these experiments

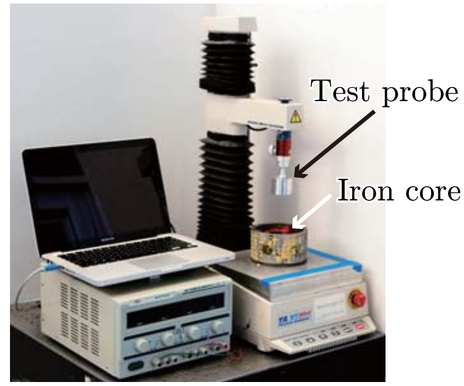

Fig. 3. Experimental apparatus for normal stress test

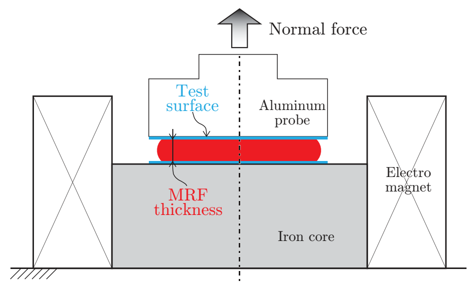

Fig. 4. Model of normal stress test

was the same LORD MRF-312DF used in [9] and [10]. The following procedure was performed for each test:

1) Select a probe surface material and roughness, and parallelize the probe with the electromagnet face to make uniform fluid thickness.
2) Using a pipette and mass scale, deposit a known quantity of MRF on the smooth steel electromagnet face.
3) Manually lower the probe until the MRF spreads to a diameter of 25 mm, as calculated from the mass and datasheet density.
4) Activate the MRF with desired magnetic flux density.
5) Measure normal adhesion force by raising the probe perpendicularly from the target surface at a rate of 10 μm/s until the fluid breaks.
6) Normalize the maximum normal adhesion force to a normal stress and save each yield normal stress.

This procedure was repeated for a variety of initial fluid thicknesses and flux densities.

B. Experimental results

The normal yield stresses are plotted as a function of initial MRF thickness, organized by magnetic flux density as shown in Fig. 5. From this figure, it is apparent that there are two distinct failure mechanisms in operation. At low flux densities, the adhesive stress is inversely proportional to the MRF thickness, but between 0.09 T and 0.12 T the adhesive stress saturates at approximately 25-30 kPa and did not increase with higher flux densities. Increasing the flux density beyond this point has very little (or even a

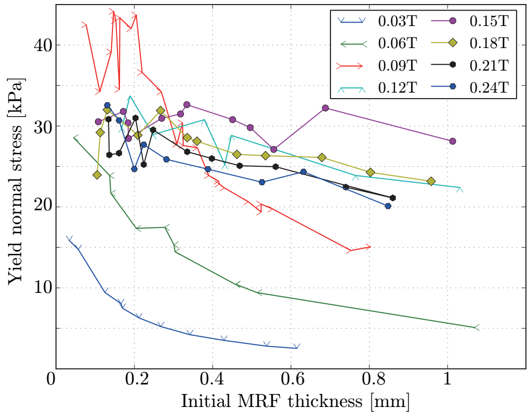

Fig. 5. Yield normal stress between smooth steel and smooth aluminum.

detrimental) effect upon the adhesive stress, and the initial MRF thickness becomes irrelevant. In fluid samples activated with magnetic flux densities below 0.12 T, the fluid failed cohesively; that is, the fluid yielded internally and flowed according to the modified Stefan adhesion model reported in [11], [12]. From these results, 0.1 T was chosen as the minimum useful flux density in order to maximize the available adhesive stress and eliminate the dependency upon the fluid thickness.

The results of the experiments using different probe materials with fluid activated with a 0.15 T flux density are shown in Fig. 6. This maximum adhesive force was found to vary little with surface roughness, surface energy, or initial fluid thickness; aluminum, sandpaper, and Teflon probes were all used in experiments on the highly-activated fluid with similar results. Of the surfaces and materials tested, the rough aluminum had the strongest adhesion, but even the rough sandpaper had an adhesive stress above 20 kPa.

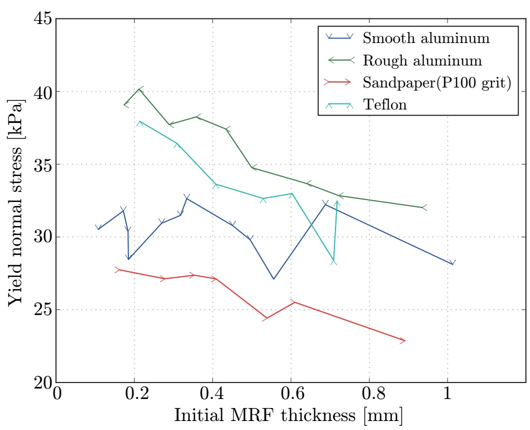

Fig. 6. Yield normal stress of MRF activated with 0.15 T with various roughnesses and materials.

III. Shear Stress Test

A. Measurement device and its model

The same probe-tack machine and a modified electromagnet were used to test the shear adhesive force of the activated MRF. A coil holder with a 1-axis linear stage was designed to hold the top surface of the electromagnet core parallel to the test probe, as shown in Fig. 7 and 8. As the steel core

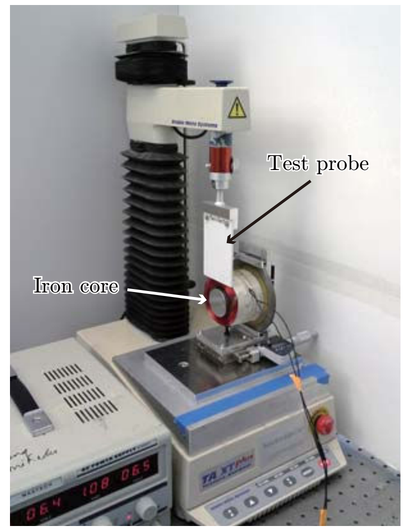

Fig. 7. Experimental apparatus for shear stress test

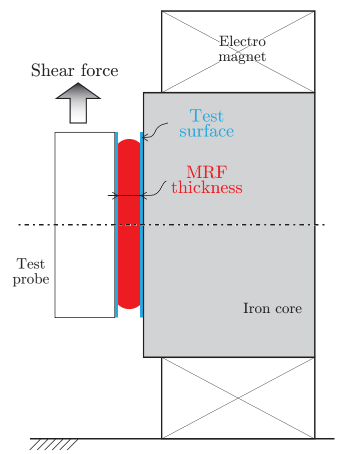

Fig. 8. Model of shear stress test

of the electromagnet was modified from the configuration used in the normal stress tests, the maximum magnetic flux density diminished to 0.18 T in this configuration.

The same experimental procedure as detailed in Section II-A was performed for each shear test, with two exceptions. First, the linear stage was moved to set the initial height of the fluid thickness, not the probe. Second, as the electromagnet face was vertical throughout each test, the MRF was held in place during assembly with a weak magnetic field. Once the electromagnet and probe were brought together, the electromagnet was briefly deactivated to allow the MRF to cleanly wet both surfaces before data collection began.

B. Experimental results

The following figures show the results of shear stress test with different magnetic field strength, MRF thickness and surface conditions. Fig. 9 shows adhesion between smooth iron and smooth aluminum. Fig. 10 shows adhesion measured between iron and P100 grit sandpaper. in every case the shear stresses were less than 10 % of yield normal stress; however, these shear stresses were shown to increase with both increased MRF thickness and increased field strength. By comparing lines of equal flux density between the two

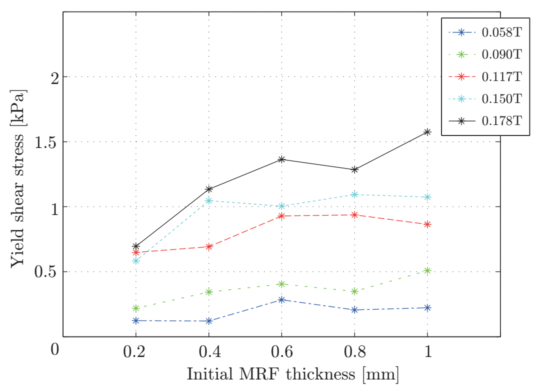

Fig. 9. Result of shear stress tests between iron and aluminum.

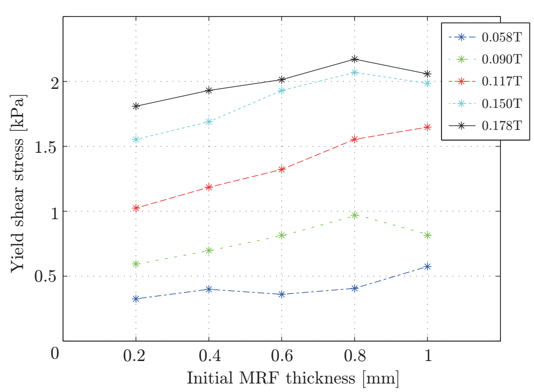

Fig. 10. Result of shear stress test between iron and P100 grit sandpaper.

figures, it is clear that roughness increases the yield shear stress of the MRF; the results in Fig. 10 are roughly twice as strong as those in Fig. 9.

IV. Adhesion control of robot for climbing on vertical wall

A. Experimental setup

Based on the experimental results of the previous sections, the four-legged climbing robot as shown in Fig. 11 was designed. The robot is 271 mm long, 234 mm wide, and 65 mm tall, and has a mass of 1.26 kg. The robot has 12 servo motors, 3 for each leg, to actuate each leg and magnet joints as shown in Fig. 12. The elbow joint (a) moves the robot's foot forward and backward in a nearly straight line through a

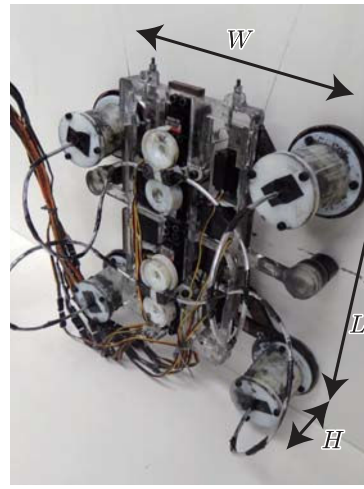

Fig. 11. Four legged climbing robot system

Chebyshev linkage. The foot rotates freely, because it is not hold rigidly by the linkage. The shoulder joint (b) moves the foot toward and away from the wall. The magnet manipulator (c) actuates a permanent magnet toward and away from the foot's sole via a steel cable routed through stiff aluminum tubes at the top of the foot. The cable is driven by a spoller motor mechanism to pull and push to a desired location. Based on the results of shear testing, half of each foot sole are covered by sandpaper (P320 grit) as shown in Fig. 13. The space, which is not covered with sand paper, aimed to hold more MRF, because shear stress increases according to thickness of MRF. For maximum adhesion, only one leg

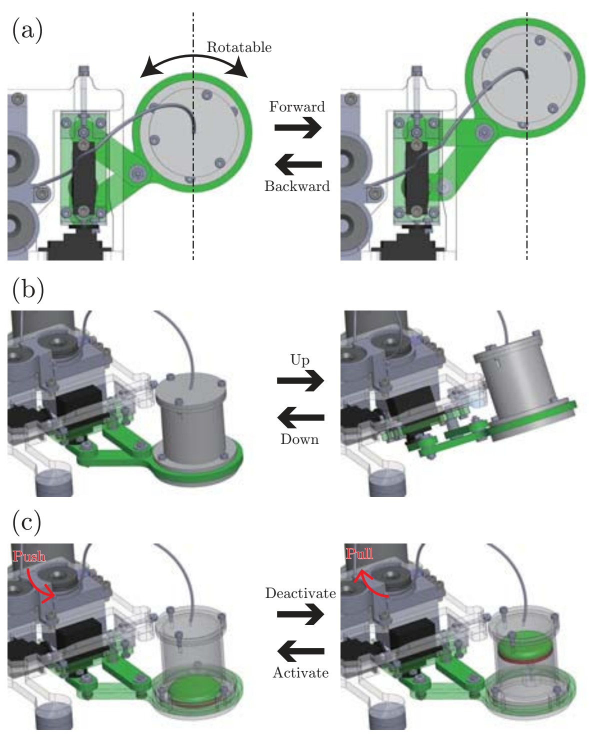

Fig. 12. Motion direction of leg and magnet joints

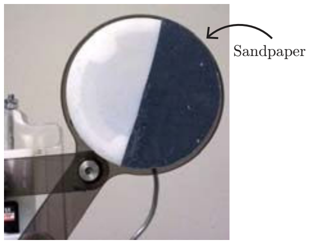

Fig. 13. View of the foot sole from bottom side

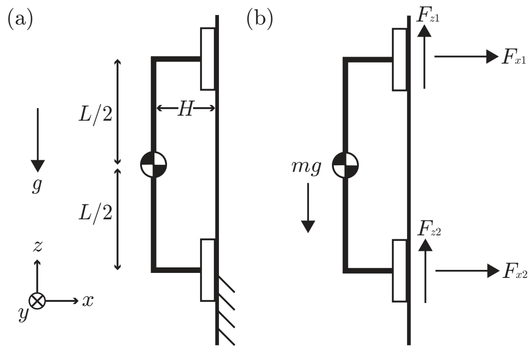

Fig. 14. Model of the climbing robot in sagittal plane

is moved at a time in a tripod gait. The legs move in the sequence RIGHT-FRONT ⇒ LEFT-FRONT ⇒ LEFT-REAR ⇒ RIGHT-REAR (⇒ RIGHT-FRONT ...).

B. Feasibility study

The climbing robot was modeled as a planar static linkage, as shown in Fig. 14, where m and g represent mass and gravity, and $F_{x1},\ F_{x2}$ and $F_{z1},\ F_{z2}$ are the reaction forces from the wall for the x and z axis directions, respectively. When the robot is adhered to the wall, the static force and moment balances result in the relationships:

$$\left\{ \begin{array}{l} F_{x1} = -F_{x2} \\ F_{z1} + F_{z2} = mg \\ F_{x1} = \frac{mgH}{L} \end{array} \right. \tag{1}$$

In analyzing the expected state of stress across the robot's feet, the observation made by Tang *et al.* [13] was utilized. Tang observed that the effective shear stress in an MRF tends to increase with an increasing compressive force. This observation implies that, since the rear legs are constantly in compression, the observed yield shear stress at the rear legs will be higher than that at the front legs. The robot, therefore, will experience the least shear resistance when one of rear legs is moving and deactivated. The following feasibility study thus employs the two assumptions. One is that the robot adheres to the wall with two front legs and one rear leg. The other is that field strength is divided into five areas(area1:0.058[T] - 0.09, area2: 0.09 - 0.117, area3: 0.117 - 0.15, area4: 0.15 - 0.178, area5: over 0.178) and then approximated yield shear stresses are selected most smallest values (0.33 kPa, 0.60, 1.0, 1.6 and 1.8) as representative values based on the Fig. 10. Tang *et al.* [13] report that the compression-modified yield shear stress, τ_c, can be found as:

$$\tau_c = \tau + KP \tag{2}$$

where K and P are a proportional constant and the compression stress, respectively. Here, K was empirically measured with some magnetic field strengths. One difference is that volume fraction of iron particle in their MRF is 46-50 %, but MRF-132DF has 70%. So we assume that this difference does not affect significantly, and then we estimate new Ks foe each representative values as shown in Fig. 15. Red $*$, Black dashed line and Blue dots mean K values in [13], linear approximation of them and estimated coefficient values.

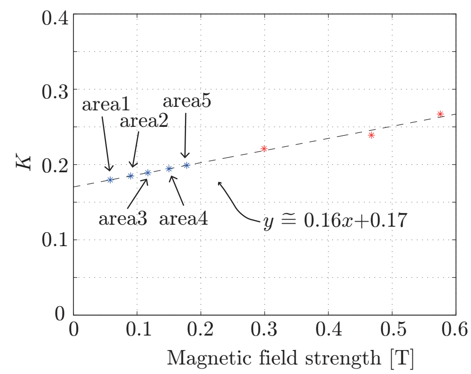

Fig. 15. Relationship between field strength and proportional value K [13]

Based on (1) and (2), 42 grade neodymium permanent magnets were chosen with a 38.1 mm diameter and 3.2 mm thickness, as shown in Fig. 16(a). Fig. 16(b) also shows an analysis of magnetic flux density on the surface of the magnet as a function of radius by FEMM software. As the magnet generates a flux density in each area, the MRF fluid is "activated" with respect to each yield shear stress. Over 24.9 mm area(no colored) is not used in this feasibility study. The estimated adhesion force in the normal direction predicts that the robot can keep its body on the wall. On the other hand, the estimated adhesion in the shear direction is 8.6 N which is slightly smaller than robot loading(12.4 N). However, the magnet configuration is actually sufficient with any three of four legs as shown in the section IV-C, because we didn't modeled some factors such as friction between foot and wall, and MRF thickness under the foot. In both cases, those factors causes more forces in the shear direction.

C. Experiment on vertical wall

The robot's climbing performance was tested on a vertical wall covered in P320 grit sandpaper. Fig. 17 shows the sequence of climbing motion. Note that in this experiment MRF was manually supplied to each foot before activation, because this robot does not have any fluid supply mechanism, such as a tank and pump and it helps for filling the empty space under the foot. The climbing robot could climb 3

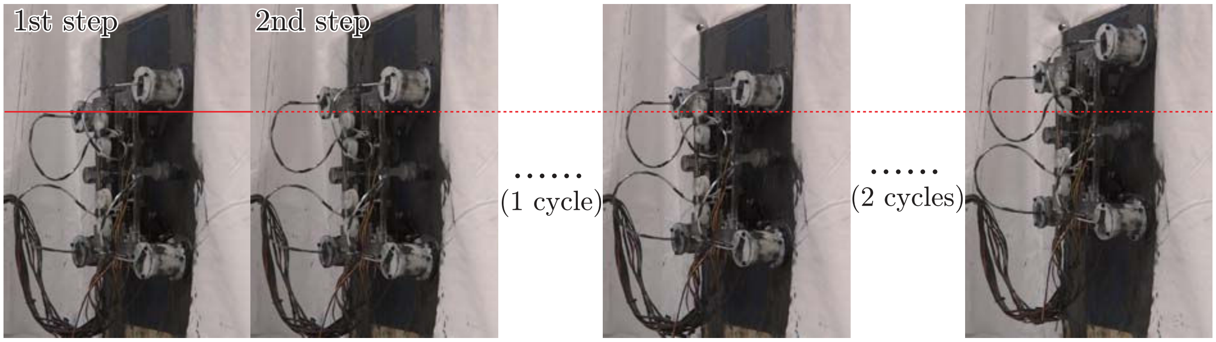

Fig. 17. Robot locomotion on rough vertical wall

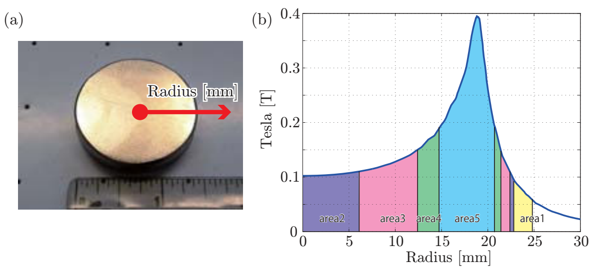

Fig. 16. Analysis of flux density of the neodymium magnet

cycles with about 1.4 mm/sec on the wall smoothly, so this result represents the effectiveness of the climbing technology using MRF for rough and dusty surface. The locomotion speed is limited by current mechanical design. At least, three of the foots are required to hold on the wall, so the control strategy have to move each leg in order. The MRF activation/deactivation time occurs on the order of milliseconds [14].

V. Conclusion

We have explored the characteristics of the field-activated MRF with various conditions, and developed a robot which could climb on rough wall. The results of this paper are as follows;

1) For flux densities greater than 0.1 T, yield normal stress saturates between 25 to 30 kPa. Increasing the flux density beyond this point does not increase the maximum stress. Surface material and roughness influence the yield normal stress, but even rough sandpaper exceeds 20 kPa.
2) Yield shear stress increases according to strength of magnetic field. Rough surfaces exhibit larger yield stresses, with sandpaper capable of maintaining twice the stress of smooth surfaces.
3) The explored characteristics were applied to design a new four-legged robot capable of climbing walls. This robot is capable of climbing on rough walls continuously, demonstrating the effectiveness of MRF controllable adhesion for non-ferromagnetic and rough surfaces.

References

[1] M. Sitti and R. S. Fearing, "Synthetic gecko foot-hair micro nano-structures as dry adhesives," *Journal of Adhesion Science and Technology*, vol. 17, no. 8, pp. 1055–1073, 2003.

[2] D. Santos *et al.*, "Gecko-inspired climbing behaviors on vertical and overhanging surfaces," in *Proc. of the 2008 IEEE Intl. Conference on Robotics and*, May 2008, pp. 1125 –1131.

[3] M. J. Spenko *et al.*, "Biologically inspired climbing with a hexapedal robot," *Journal of Field Robotics*, vol. 25, no. 4-5, pp. 223–242, April 2008.

[4] K. Daltorio *et al.*, "A small wall-walking robot with compliant, adhesive feet," in *Proc. of the 2005 IEEE/RSJ Intl. Conference on Intelligent Robots and Systems*, Aug. 2005, pp. 3648 – 3653.

[5] H. Prahlad *et al.*, "Electroadhesive robots - wall climbing robots enabled by a novel, robust, and electrically controllable adhesion technology," in *Proc. of the 2008 IEEE Intl. Conference on Robotics and Automation*, May 2008, pp. 3028 –3033.

[6] S. Kitai, K. Tsuru, and S. Hirose, "The proposal of swarm type wall climbing robot system "anchor climber"," in *Proc. of the 2005 IEEE/RSJ Intl. Conference on Intelligent Robots and Systems*, Aug. 2005, pp. 475 –480.

[7] A. Nagakubo and S. Hirose, "Walking and running of the quadruped wall-climbing robot," in *Proc. of the 1994 IEEE Intl. Conference on Robotics and Automation*, May 1994, pp. 1005 –1012 vol.2.

[8] Y. Yoshida and S. Ma, "A wall-climbing robot without any active suction mechanisms," in *Proc. of the 2011 IEEE Intl. Conference on Robotics and Biomimetics*, Dec. 2011, pp. 2014 –2019.

[9] R. H. Ewoldt, P. Tourkine, G. H. McKinley, and A. E. Hosoi, "Controllable adhesion using field-activated fluids," *Physics of Fluids*, vol. 23, no. 7, 2011.

[10] N. Wiltsie, M. Lanzetta, and K. Iagnemma, "A controllably adhesive climbing robot using magnetorheological fluid," in *Proc. of the 2012 IEEE Intl. Conference on Technologies for Practical Robot Applications*, April 2012, pp. 91–96.

[11] A. M. Smith, "The structure and function of adhesive gels from invertebrates," *Integrative and Comparative Biology*, vol. 42, no. 6, pp. 1164–1171, 2002.

[12] N. Wiltsie, "A controllably adhesive climbing robot using magnetorheological fluid," Master's thesis, Massachusetts Institute of Technology, Cambridge, 2012.

[13] X. Tang, X. Zhang, R. Tao, and Y. Rong, "Structure-enhanced yield stress of magnetorheological fluids," *Journal of Applied Physics*, vol. 87, no. 5, 2000.

[14] H. Laun and C. Gabriel, "Measurement modes of the response time of a magneto-rheological fluid (mrf) for changing magnetic flux density," *Rheologica Acta*, vol. 46, pp. 665–676, 2007.